Antiviral Research 98 (2013) 144–152

Contents lists available at SciVerse ScienceDirect

Antiviral Research

journal homepage: www.elsevier.com/locate/antiviral

Inhibition of hepatitis C viral RNA-dependent RNA polymerase by α-*P*-boranophosphate nucleotides: Exploring a potential strategy for mechanism-based HCV drug design

Marcus Adrian Cheek *, Mariam L. Sharaf, Mikhail I. Dobrikov, Barbara Ramsay Shaw

Department of Chemistry, Duke University, P.O. Box 90346 Durham, NC 27708-0346, United States

ARTICLE INFO

Article history:
Received 21 September 2012
Revised 2 February 2013
Accepted 21 February 2013
Available online 4 March 2013

Keywords:
Boranophosphate
Hepatitis C virus
Enzyme kinetics
Boron
R_p-5′-(α-*P*-borano) nucleoside triphosphate
NS5BΔ55

ABSTRACT

Improved treatments for chronic HCV infections remain a challenge, and new chemical strategies are needed to expand the current paradigm. The HCV RNA polymerase (RdRP) has been a target for antiviral development. For the first time we show that the boranophosphate (BP) modification increases the substrate efficiency of ATP analogs into HCV NS5BΔ55 RdRP-catalyzed RNA. Boranophosphate nucleotides contain a borane (BH_3) group substituted for a non-bridging phosphoryl oxygen of a normal phosphate group, resulting in a class of modified isoelectronic DNA and RNA mimics capable of modulating the reading and writing of genetic information. We determine that HCV NS5BΔ55, being a stereospecific enzyme, incorporates the R_p isomer of both ATPαB and the two boranophosphate analogs: 2′-*O*-methyladenosine 5′-(α-*P*-borano) triphosphate (2′-OMe ATPαB, **5a**) and 3′-deoxyadenosine 5′-(α-*P*-borano) triphosphate (3′-dATPαB, **5b**). The R_p diastereomer of ATPαB (**6**), having no ribose modifications, was found to be a slightly better substrate than natural ATP, showing a 42% decrease in the apparent Michaelis–Menten constant (K_m). The IC_{50} of both 2′-*O*-Me and 3′-deoxy ATP was decreased with the boranophosphate modification up to 16-fold. This "borano effect" was further confirmed by determining the steady-state inhibitory constant (K_i), showing a comparable potency shift (21-fold). These experiments also indicate that the boranophosphate analogs **5a** and **5b** inhibit HCV NS5B through a competitive mode of inhibition. This evidence, together with previous crystal structure data, further supports the idea that HCV NS5B (in a similar manner to HIV-1 RT) discriminates against the 3′-deoxy modification via lost interactions between the 3′-OH on the ribose and the active site residues, or lost intramolecular hydrogen bonding interactions between the 3′-OH and the pyrophosphate leaving group during phosphoryl transfer. To our knowledge, these data represent the first time a phosphate modified NTP has been studied as a substrate for HCV NS5B RdRP.

1. Introduction

Hepatitis C virus (HCV) is known to persistently infect 170 million people worldwide and is one of the leading causes of cirrhosis (WHO, 1999). Additionally, 40% of all HCV-related deaths are due to the development of hepatocellular carcinoma (Sangiovanni et al., 2006). Currently the primary FDA approved treatment for HCV infection involves a combination of ribavirin and pegylated interferon α2b, which is approximately 40–80% effective depending on viral genotype (Fried et al., 2002). Protease inhibitors Boceprevir or Telaprevir can be added to improve antiviral response for hepatitis C genotype 1 (Ghany et al., 2011).

HCV is a positive strand RNA virus containing a genome of approximately 9.6 kb (Takamizawa et al., 1991). During the last decade, the nonstructural protein 5B (NS5B), an RNA dependent RNA polymerase (RdRP) that is responsible for genome replication, has become an attractive target for nucleoside based inhibitors (Behrens et al., 1996; Lohmann et al., 1997; Penin et al., 2004; Powdrill et al., 2010; Sofia et al., 2011). Current literature has revealed a variety of sugar-modified chain terminating nucleosides that target the HCV NS5B with varying efficacy including: 2′-O-methyl, 2′-C-methyl, 4′-azido, 3′-deoxy, and 2′-fluoro-2′-C-methyl NTPs (Carroll et al., 2009, 2003; Deval et al., 2007; Mosley et al., 2012; Murakami et al., 2007; Olsen et al., 2004; Shim et al., 2003). Due to the similarities between the palm domains of human immunodeficiency virus reverse transcriptase (HIV-RT) and that of HCV NS5B RdRP, and the success of chain terminating nucleoside reverse transcriptase inhibitors (NRTIs)

* Corresponding authors. Tel.: +1 919 660 1551.
E-mail addresses: marcus.cheek@duke.edu (M.A. Cheek), barbara.ramsay.shaw@duke.edu (B.R. Shaw).

0166-3542/$ - see front matter © 2013 Elsevier B.V. All rights reserved.
http://dx.doi.org/10.1016/j.antiviral.2013.02.014

targeting HIV-RT (Bressanelli et al., 1999; De Clercq, 2009), it is not surprising that nucleoside-based NS5B inhibitors are being heavily investigated.

Of particular interest to our group is understanding the effects that 5′-(α-*P*-borano) nucleoside triphosphates (NTPαBs) can exert on viral polymerase activity (Fig. 1).

The boranophosphate modification, where one non-bridging α-phosphate oxygen is replaced by a borane group (BH_3), confers unique properties to ribonucleoside triphosphates (NTPs). Specifically, borane contains a less electronegative boron (2.04) in comparison to oxygen (3.44), and would rather occupy the equatorial position in a trigonal bipyramidal complex during SN_2-like nucleophilic substitutions (i.e. BH_3 would have lower apicophilicity than oxygen) (Sood et al., 1990; Thatcher and Campbell, 1993). This lower apicophilicity is important considering that RNA polymerases purportedly facilitate the addition of NTP's to a growing strand via a trigonal bipyramidal transition state (Brautigam and Steitz, 1998). The BH_3 group of an R_p-NTPαB involved in this transition state would likely not interact with Mg^{2+}, and therefore not interfere with the inline attack coordinate along the two apical bonds. Additionally, as hypothesized by our lab and others, the pyrophosphate (PPi) group on an NTPαB would be a more efficient leaving group compared with natural NTPs, due to more electron density on the α-phosphorus. Furthermore, the remaining non-bridging α-*P*-oxygen on the NTPαB should retain more electron density and coordinate more strongly to metal ions (Mg^{2+} or Mn^{2+}) in the polymerase active site (Deval et al., 2005; Summers et al., 2001). Therefore, we proposed that the unique chemistry of boranophosphates might increase the efficacy of chain terminating nucleotide incorporation into RNA by HCV polymerase (NS5BΔ55).

NTPαBs have been shown to be efficient and selective substrates for wild-type (wt) and, to a greater extent, drug-resistant viral reverse transcriptases (Li et al., 2007; Shaw et al., 2003). The R_p stereoisomer of ddCTPαB was shown to be incorporated into drug-resistant MMLV RT 28-fold more efficiently than ddCTP (Dobrikov et al., 2003). Additionally, against drug-resistant HIV-1 RT, the R_p stereoisomer of AZTTPαB, D4TTPαB, and ddATPαB all exhibited dramatic increases in potency when compared to natural phosphate controls (Deval et al., 2005; Meyer et al., 2000; Selmi et al., 2001).

Here we investigated, for the first time, the inhibition of HCV NS5B RdRP by two new α-*P*-borano modified nucleotide analogs: 2′-O-methyladenosine 5′-(α-*P*-borano) triphosphate (2′-OMe ATPαB, **5a**) and 3′-deoxyadenosine 5′-(α-*P*-borano) triphosphate (3′-dATPαB, **5b**) (Fig. 2). Following the synthesis, purification, and characterization of the R_p and S_p diastereomers of both nucleotides, the inhibitory concentration 50% (IC_{50}) and steady state inhibition constant (K_i) were determined and compared to the non-boronated controls. Additionally, we studied the steady state kinetics of ATPαB (**6**) incorporation to further characterize the effect of this unique boron modification.

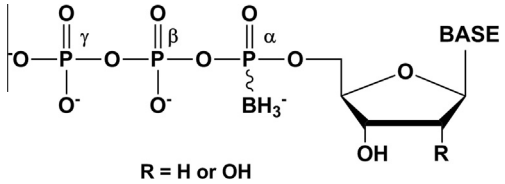

Fig. 1. Generic structure of 2′-deoxy-NTPαB (*R* = H) or ribo-NTPαB (*R* = OH) with *R*, *S* stereochemistry on the α-phosphorus.

2. Materials and methods

2.1. Materials

HCV NS5BΔ55 and heteropolymeric RNA template (t500) were generously provided by Merck & Co., Inc. The t500 RNA template was generated via runoff transcription as previously described and corresponds to base numbers 3504–4004 of the BK genome (Carroll et al., 2000; Takamizawa et al., 1991). HCV (BK strain) NS5BΔ55 was expressed in *Escherichia coli* BL21(DE3) harboring plasmid pT7(NS5BΔ55) and purified as previously described (Carroll et al., 2003). All natural NTPs were purchased from Promega. 2′ and 3′-modified nucleosides were purchased from Berry's and Associates. 2′ and 3′-modified NTP controls were purchased from Trilink. ATPαB was synthesized and purified as previously described (He et al., 1998). UV spectra were obtained on a Nanodrop UV apparatus. NMR spectra were recorded on a Varian-Inova 400 spectrometer, and chemical shift values (δ) are relative to tetramethylsilane (TMS) for ^1H NMR or H_3PO_4 for ^{31}P NMR. All other reagents were available from Sigma–Aldrich, Acros, or Ambion. The detailed synthesis of ATP analogs 2′-OMe ATPαB (**5a)** and 3′-dATPαB (**5b**) can be found in supplementary material.

2.2. Steady-state kinetics using t500 RNA Template

Unless otherwise noted, NS5BΔ55-catalyzed reactions contained 25 nM or 75 nM NS5BΔ55 in a 20 μL reaction consisting of 90 nM t500 RNA template, 20 mM Tris, pH 7.5, 80 mM KCl, 4 mM MgCl, 5 mM DTT, 0.4 unit/μL RNasin (Promega), 0.2% polyethylene glycol 8000, 50 μM EDTA; 1 μM NTPs (IC_{50} determination), or ATP was varied and 100 μM GTP, CTP, ~1–2 μCi of [α-^{33}P]UTP and 10 μM UTP (K_i determination). RNA template was preincubated for 30 min in the reaction stock and then added to the NTP mixture pre-aliquoted into a 96-well plate to initiate the reaction. At the desired time point, the reactions were quenched with 0.5 M EDTA and aliquots were spotted onto Whatman DE-81 25 mm filter disks. After drying, the filters were washed in 0.3 M ammonium formate buffer five times for 10 min. Spotted unwashed filters were used to determine specific activity. Filters were counted in 4.5 mL Safety-Solv (RPI Corp.) scintillation fluid in a Beckman LS 6000 Scintillation Counter. Reaction times were chosen from the linear region of the time course experiments initially performed.

2.3. Data analysis

All data was analyzed using Graphpad Prism 5 software. The inhibitor concentration which reduces the polymerase activity to 50% (IC_{50}) was determined using the Hill equation, $Y = \%Min + (\%Max - \%Min)/(1 + 10^{((LogIC_{50} - X)*HillSlope)})$ where *Y* is the percent enzyme activity, *X* is the Log_{10} of inhibitor concentrations, and %Min and %Max are the bottom and top asymptotes respectively with the same units as *Y*. IC_{50} values were determined by a minimum of three independent experiments. The apparent Michaelis–Menten constant (K_m) and maximum velocity (V_{max}) values for natural NTPs and ATPαB were calculated by fitting data to the Henri-Michaelis–Menten hyperbolic equation, $Y = V_{max}*X/(K_m + X)$ where *Y* is the initial velocity of RNA synthesis, and X is the NTP concentration in μM. The steady-state inhibition constant (K_i in μM) of each inhibitor was calculated by nonlinear fitting of data to the following equations (assuming a competitive mechanism): $Y = V_{max}*X/(K_mObs + X)$ and $K_mObs = K_m*(1 + [I]/K_i)$ where $[I]$ is the concentration of the inhibitor in μM, and *X* is the concentration of ATP in μM. K_i values were determined by a minimum of three independent experiments. Lineweaver–Burk plots are shown for

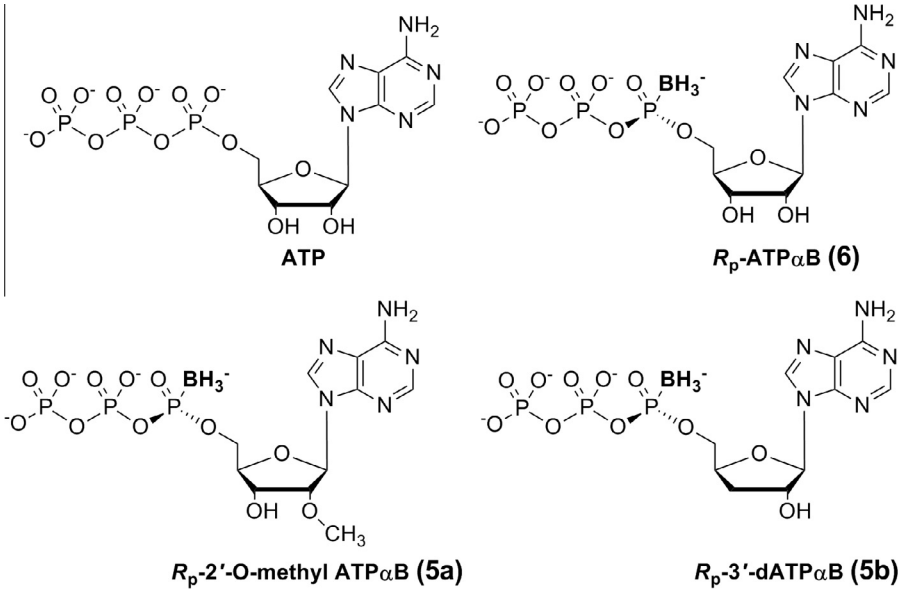

Fig. 2. Structures of the R_p diastereomers of 2′-OMe ATPαB (**5a**), 3′-dATPαB (**5b**), ATPαB (**6**), along with ATP showing an achiral α-phosphorus.

qualitative purposes only. The K_i for each compound was initially approximated using the Cheng-Prusoff equation, $K_i = IC_{50}/(1 + [ATP]/K_m)$, where [ATP] is the concentration of ATP in the dose-dependent experiments (1 μM) (Cheng and Prusoff, 1973). The concentration of inhibitor in the competitive inhibition assays was set at approximately $10K_i$ and then serially diluted to span the initially calculated Cheng-Prusoff K_i.

3. Results

3.1. Synthesis of NTPαBs

The syntheses of 2′-OMe ATPαB (**5a**) and 3′-dATPαB, (**5b**) are shown in Fig. 3. Commercially available nucleosides **1a** and **1b** were converted to the acetylated derivatives N^4-acetyl, 3′-O-acetyl, 2′-O-methyladenosine (**4a**) and N^4-acetyl, 2′-O-acetyl, 3′-deoxyadenosine (**4b**), respectively, via silylation of the 5′-hydroxyl with *tert*-butyldiphenylchlorosilane (TBDPS-Cl) in the presence of imidazole in DMF to give **2a** or **2b**, followed by acetylation of the exocyclic amine and the remaining secondary sugar hydroxyl with an excess of acetic anhydride in pyridine and CH_2Cl_2 to give **3a** or **3b**. The 5′-O-TBDPS group was removed using TEA·3HF in THF overnight to give **4a** or **4b** in 66% and 56% yield respectively. TEA·3HF provided a much less reactive fluoride source than the traditional tetrabutylammonium fluoride (TBAF) deblocking reagent, producing fewer byproducts, and increasing the overall yield (Westman and Strömberg, 1994).

NTPαB analogues **5a**, **5b** and ATPαB (**6**) were synthesized via a one pot synthesis previously developed by our lab in 27% and 30% overall yield, respectively (He et al., 1998). Alterations to the original synthesis include: the use of borane-dimethylsulfide com-

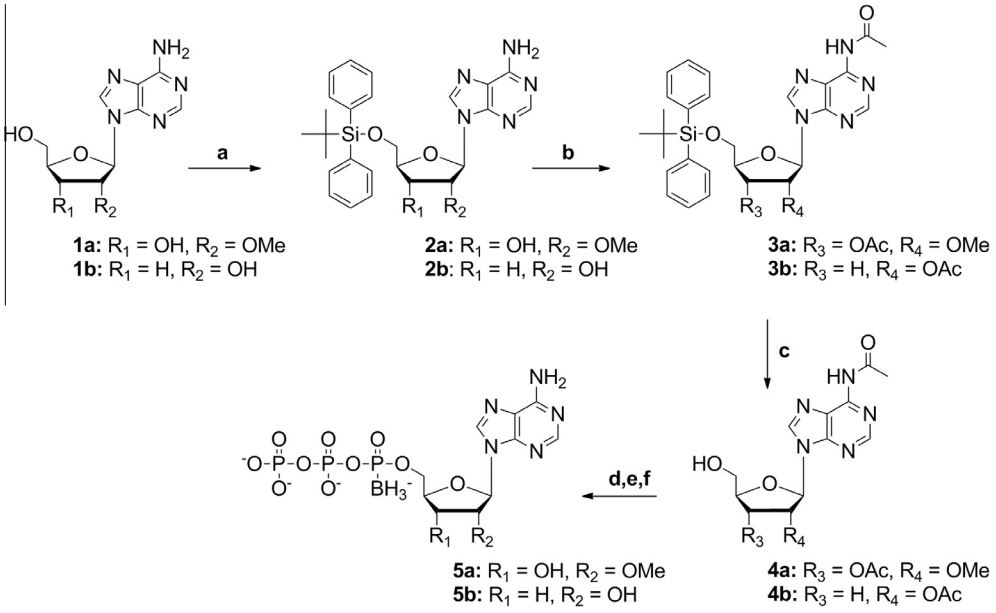

Fig. 3. Synthesis of ATPαB analogs. Reagents: (a) TBDPS-Cl, imidazole, DMF, −5 °C; (b) acetic anhydride, pyridine, CH_2Cl_2; (c) TEA·3HF, THF; (d) 2-chloro-4H-1,2,3-benzodioxaphosporin-4-one, 0.5 M tributylammonium pyrophosphate, tributylamine, 2.0 M $SMe_2{\cdot}BH_3$ in THF; (e) TEA:H_2O (3:2); (f) NH_4OH, 50 °C.

plex ($SMe_2{\cdot}BH_3$) during the boronation step in place of borane-diisopropylethylamine complex ($DIPEA{\cdot}BH_3$), and a 3:2 mixture of triethylamine and water for the hydrolysis step instead of aqueous ammonium hydroxide (NH_3OH). Both procedural modifications cut the reaction times significantly and did not significantly affect the yields. Stereoisomers of **5a**, **5b**, and **6** were each separated and purified using reverse phase HPLC (under ion pairing conditions) and isolated as the triethylammonium salt. For a more detailed accounting of the NTPαB synthetic procedure see the supplementary material section.

3.2. NS5BΔ55 prefers the R_p stereoisomer

To understand how NTPαB analogs **5a** and **5b** might affect HCV NS5B-catalyzed RNA chain elongation, a standard *in vitro* RNA filter binding assay was utilized where a 500 nucleotide heteropolymeric RNA template (t500) produces a hairpin product via a copy-back mechanism (De Francesco et al., 1996). Chain elongation was quantified by measuring the incorporated [α-^{33}P]UTP by spotting aliquots of the reaction mixture onto cationic DE-81 filter disks, which retain only the radiolabeled elongated RNA products after washing with ammonium formate buffer (Behrens et al., 1996; Bryant et al., 1983; Carroll et al., 2000). The NS5BΔ55-catalyzed product formation followed a typical biphasic time course including a burst phase followed by a slower linear phase (Fig. 4).

To visualize the RNA products formed during a typical enzymatic reaction, selected reaction mixtures containing: 100 nM NS5BΔ55, 100 nM t500 RNA template, with 500 μM ATP, CTP, and UTP and 10 μM GTP and 5 μCi of [α-^{32}P]GTP, in RdRP buffer were incubated for 45 min and quenched with 0.5 M EDTA. An aliquot was then diluted with formamide running buffer, loaded onto a 5% polyacrylamide gel (PAGE) containing 8 M urea, and imaged on a phosphorimager followed by ethidium bromide visualization (supplementary material, Fig. 1). The RNA template and product sizes were compared with RNA standards of known lengths. The PAGE gel of the reaction mixture confirmed that the copy-back product, running at approximately the same rate as a ~200 nt RNA strand, was the major product formed from the 500 nt template. This is consistent with previous observations of reactions run under the same conditions containing the same enzyme and template (Carroll et al., 2000; De Francesco et al., 1996).

The steady-state constants for each of the four natural NTPs (Fig. 5) were determined by successively varying the concentration of one NTP while measuring the total incorporation of radiolabeled UMP (or GTP) at a reaction time that corresponds to the linear region of the time course. The other three NTPs were held at concentrations above their respective K_m values, which were determined through multiple reiterations. Additionally, the steady-state constants for R_p-ATPαB (**6**) were determined using the same conditions as above (Fig. 6).

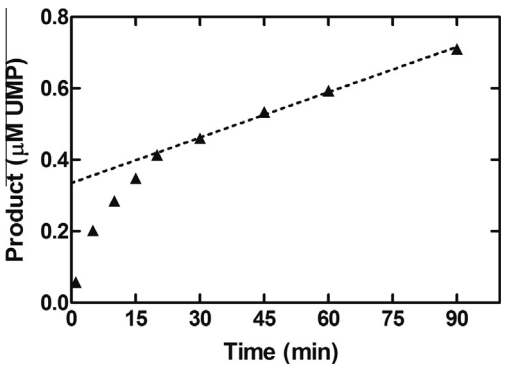

Fig. 4. A representative biphasic time dependent reaction progress curve showing a steady-state region beginning at approximately 20 min. NS5BΔ55-catalysed reaction carried out using 100 nM t500 RNA template with 10 μM UTP, 100 μM ATP, GTP and CTP as described in the material and methods Section 2. 2**.** Many such time courses were performed and generated an optimal linear region between 20 and 90 min as shown here.

As seen in Table 1, catalytic efficiency (k_{cat}/K_m) of each NTP substrate implies that HCV NS5BΔ55 selectivity follows the trend: CTP > UTP > GTP > R_p-ATPαB (**6**) > ATP, where CTP is the best and natural ATP is the worst substrate respectively. The S_p isomer of ATPαB was found not to be a substrate of HCV NS5BΔ55.

3.3. Inhibition of NS5BΔ55 RdRP chain elongation

HCV NS5B mediated RNA synthesis in the presence of R_p-2′-OMe ATPαB, **5a** and R_p-3′-dATPαB **5b** was measured using the same DE-81 filter-binding assay utilized in the previous section. Single concentration inhibition experiments were performed initially to determine if one or both stereoisomers of **5a** and **5b** could in fact inhibit RNA synthesis. This experiment was run parallel to the normal phosphate controls set to the literature inhibitory concentrations that yield 50% polymerase activity (IC_{50}) values of 50 μM and 22 μM for 2′-OMe ATP and 3′-dATP, respectively (Olsen et al., 2004). Only the R_p stereoisomer of **5a** and **5b** showed any inhibitory activity when compared with the normal phosphate controls (data not shown). Furthermore, a much lower concentration of the R_p isomer of both **5a** and **5b** was required to inhibit HCV NS5B as compared to the experimental controls. The next step was to evaluate the inhibitory potency of **5a** and **5b** versus their natural phosphate forms in a dose-dependent experiment. All four NTPs were held at a concentration of 1 μM with a reaction time of 45 min. The HCV NS5BΔ55-catalyzed RNA product formation was determined by measuring the total incorporation of a radiolabeled nucleotide ([α-^{33}P]GTP) in the presence of increasing inhibitor concentration. The data was fitted to a four-parameter Hill equation, and the R_p isomer of both **5a** and **5b** reduced the rate of NS5B-catalyzed RNA synthesis. The Hill plots of percent polymerase activity (% Pol Activity) versus inhibitor concentration are shown in Fig. 7.

All curves generated Hill slopes close to −1 indicating no cooperativity. The stereospecificity of NS5B was further confirmed since the S_p isomer of **5a** and **5b** did not reduce polymerase activity by any appreciable amount. When compared to the natural phosphate controls, **5a** and **5b** exhibited potency shifts of 3.4 and 16-fold respectively, confirming that the R_p-α-*P*-BH_3 modification enhances the inhibitory properties of both analogs (Table 2).

3.4. NTPαB inhibitors retain a competitive mode of inhibition

Since the boranophosphate modification changes both the structural and electronic properties of a nucleoside triphosphate, it was feasible that an NTPαB could bind to the enzyme or enzyme-template complex at a location other than the active site. Such allosteric-type binding could lead to a mixed mode of inhibition, combining aspects of competitive and uncompetitive inhibition. However, one could reasonably deduce that **5a** and **5b** exhibit a competitive mode of inhibition, since ATPαB (**6**) successfully replaced ATP during NS5B-catalyzed RNA synthesis.

To determine if the α-*P*-BH_3 modification changes the mode of inhibition of 2′-O-Me ATP and 3′-dATP, reactions were carried out with varying ATP concentrations and inhibitor concentrations, while the other three NTP substrates were held above their respective K_m values. The initial velocities of reactions with and without inhibitor were plotted versus ATP concentration and fit to the hyperbolic Henri-Michaelis–Menten rate equation. Reactions in the absence of ATP but including the other three NTPs were also run at the same inhibitor concentrations to establish a true baseline. The inhibition constant (K_i) was determined by nonlinear fit-

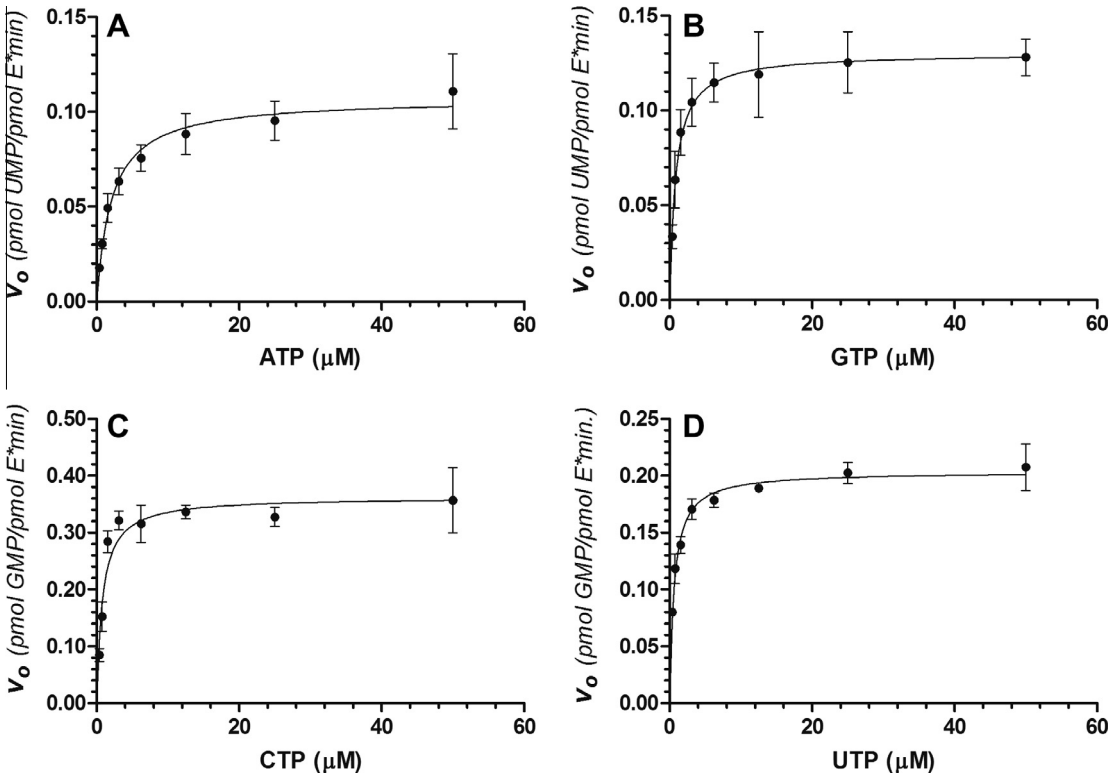

Fig. 5. Steady-state velocity curves of multiple nucleotide incorporations. Steady-state parameters were derived by non-linear fitting of data to the Henri-Michaelis–Menten equation. Rates were determined by measuring the dependence of incorporation of A) ATP (n = 7), B) GTP (n = 3), C) CTP (n = 2), and D) UTP (n = 2). [α-^{33}P]-labeled UTP was used to measure the velocities of ATP and GTP, and [α-^{33}P]-labeled GTP was used to measure the velocities of CTP and UTP.

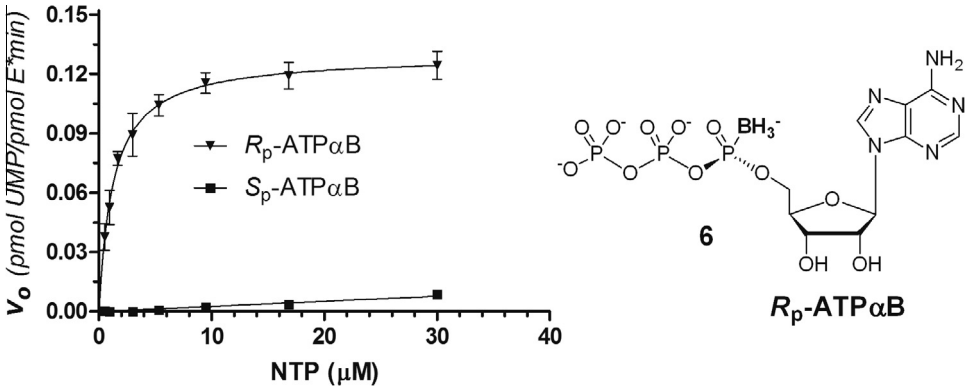

Fig. 6. Steady-state velocity curve of R_p-ATPαB (**6**) incorporation (n = 3). Data is shown for S_p-ATPαB indicating a lack of substrate recognition. Steady-state parameters were derived by non-linear fitting of data to the Henri-Michaelis–Menten equation.

Table 1
Steady-state parameters determined for R_p-ATPαB compared to NTP controls.

Nucleotide	K_m (μM)	k_{cat} (min^{-1})	k_{cat}/K_m	S[a]
R_p-ATPαB, **6** (n = 4)	1.17 ± 0.23	0.111 ± 0.037	0.095	1.7
ATP (n = 10)	2.03 ± 0.395	0.116 ± 0.018	0.057	1.0
GTP (n = 3)	0.869 ± 0.116	0.130 ± 0.013	0.150	-
CTP (n = 2)	0.804 ± 0.0001	0.363 ± 0.023	0.451	-
UTP (n = 2)	0.624 ± 0.011	0.203 ± 0.008	0.326	-

[a] Selectivity value is the ratio of catalytic efficiencies (k_{cat}/K_m) of modified NTP analogues to the natural NTP. Values greater than 1 indicate that the enzyme prefers the nucleotide analogue over the natural substrate.

ting of data from parallel experiments run at differing inhibitor concentrations as described in the material and methods Section 2.4 (Fig. 8).

Reactions were run parallel with natural phosphate controls (see supplementary material Fig. 2), and the K_i for each compound was determined from the mean of at least three independents experiments (Table 3). Lineweaver–Burk double-reciprocal plots (Fig. 8) qualitatively confirm a competitive mode of inhibition by showing convergent maximum velocities (y-intercepts) at different inhibitor concentrations. The K_i values determined for both **5a** and **5b** show a similar trend in potency shift as the IC_{50} data when compared to the natural phosphate controls. The data also show that the enzyme discriminates against all of the ATP analogues ($K_i/K_m > 1$) when compared with natural ATP, except in the case of **5b** (K_i/K_m = 0.43). Overall the data seem to imply that the R_p-α-P-BH_3 modification intrinsically increases the catalytic efficiency of both types of sugar modified NTP's. The difference in the potency shifts of **5a** (5.2-fold) and **5b** (21-fold) seems to correlate to the

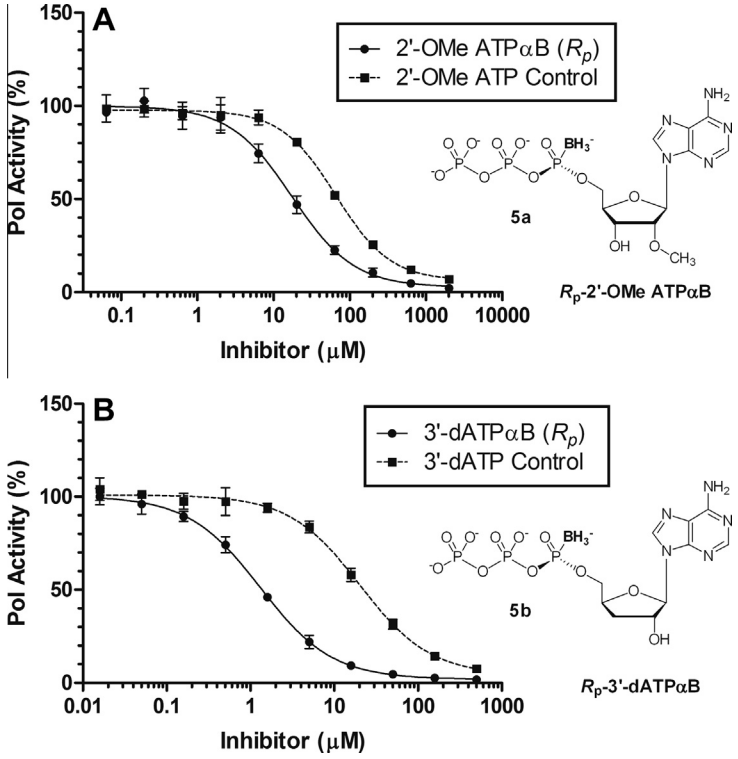

Fig. 7. Dose-dependent Hill plots showing inhibition of NS5BΔ55 in the presence of 1 μM NTPs. (A) R_p-2′-O-Me ATPαB, **5a**, and control, (B) R_p-3′-dATPαB, **5b**, and control**.** All curves generated Hill slopes close to −1 indicating no cooperativity.

Table 2
Inhibitory concentration 50% (IC_{50}) of NTPαBs and NTP controls ($n = 3$).

Inhibitor	IC_{50} (μM)	Potency Shift[a]
R_p-2′-O-Me ATPαB, **5a**	18.0 ± 3.6	3.4
2′-O-Me ATP	60.7 ± 8.5	-
R_p-3′-dATPαB, **5b**	1.31 ± 0.02	16
3′-dATP	20.4 ± 0.8	-

[a] Potency shift is the ratio of the IC_{50} of the normal phosphate control divided by the IC_{50} of the NTPαB inhibitor.

presence or absence of the ribosyl 3′-OH group. Substitution of a non-bridging α-phosphoryl oxygen with a BH_3 group exerts a four-fold greater potency shift when combined with the 3′-deoxy sugar modification as compared to 2′-O-methyl modification.

4. Discussion

We investigated, for the first time, the inhibition of HCV NS5B RNA-dependent-RNA polymerase by boranophosphate: R_p-2′-OMe ATPαB (**5a**) and R_p-3′-dATPαB, (**5b**). Knowing that the boranophosphate modification increased the incorporation of dideoxy nucleotides into HIV-1 RT (Li et al., 2007; Meyer et al., 2000), we proposed that a similar type of inhibition would occur with HCV NS5B polymerase. For HIV-1 RT, the role played by the 3′-OH of the incoming NTP for the proper positioning of the nucleotide in the active site, is well established (Selmi et al., 2001). Chain terminators lacking a 3′-OH bind to HIV-1 RT less efficiently (high K_d) due to a loss of the sugar hydroxyl interactions with proximal cationic and hydrogen-bonding residues in the active site. (Dobrikov and Shaw, 2005; Selmi et al., 2001). One could expect that this structure–activity correlation may apply to HCV NS5B because of its shared homology with HIV-1 RT.

R_p-3′-dATPαB (**5b**) was found to be a better substrate than even the natural ATP for HCV NS5BΔ55 polymerase. This is exhibited by an apparent affinity ratio (K_i/K_m (ATP)) of less than unity ($K_i/K_m = 0.43$). The boranophosphate substitution on **5b** reduced the penalty of removing the 3′-OH group from ATP by 21-fold. Further, the methyl group on 2′-OMe ATP imposed the greatest penalty to binding the E·T complex, with an apparent affinity ratio of 26.3. The boranophosphate substitution on **5a** reduced this penalty by only 5.2-fold compared to the 21-fold greater recovery in the aforementioned case of the 3'-deoxy sugar modification. Since a 3′-OH is present on 2′-OMe ATP, this would imply that the borane group is helping through another mechanism. Perhaps the bulkiness of the methoxy group at the 2′ position disrupts hydrogen-binding interactions within in the active site of the enzyme, whereas the BH_3 substitution allows for tighter binding to the catalytic Mg^{2+} ions. The crystal structure of UTP bound to manganese in the active site of NS5B shows that the conserved Asp 225 residue is in close proximity to the 2′-OH, and it is thought to occupy a similar position when NS5B is actively synthesizing RNA (Bressanelli et al., 2002; O'Farrell et al., 2003). One other important observation from the HCV NS5B crystal structure is the possible intramolecular interaction between a non-bridging pyrophosphate oxygen and 3′-OH of the bound UTP. As with the case of HIV (Selmi et al., 2001), disruption of this interaction via the removal of 3′-OH could reduce the ability for the enzyme to complete the catalytic step (Eldrup et al., 2004).

Shim et al. also studied the inhibitory properties of 3′-deoxy NTPs (N = A, G, C, or U) versus HCV NS5B (Shim et al., 2003), but they used a different RNA template and polymerase elongation assay than in our study. Depending on the nucleobase, their apparent affinity ratios (K_i/K_m (NTP)) ranged from 2–25, indicating that lack of a 3′-OH (e.g. 3′-deoxy) could affect the apparent binding of the nucleotide to the E·T complex. With this in mind, they obtained a lower apparent affinity ratio value for 3′-dATP ($K_i/K_{m(ATP)} = 2.3$)

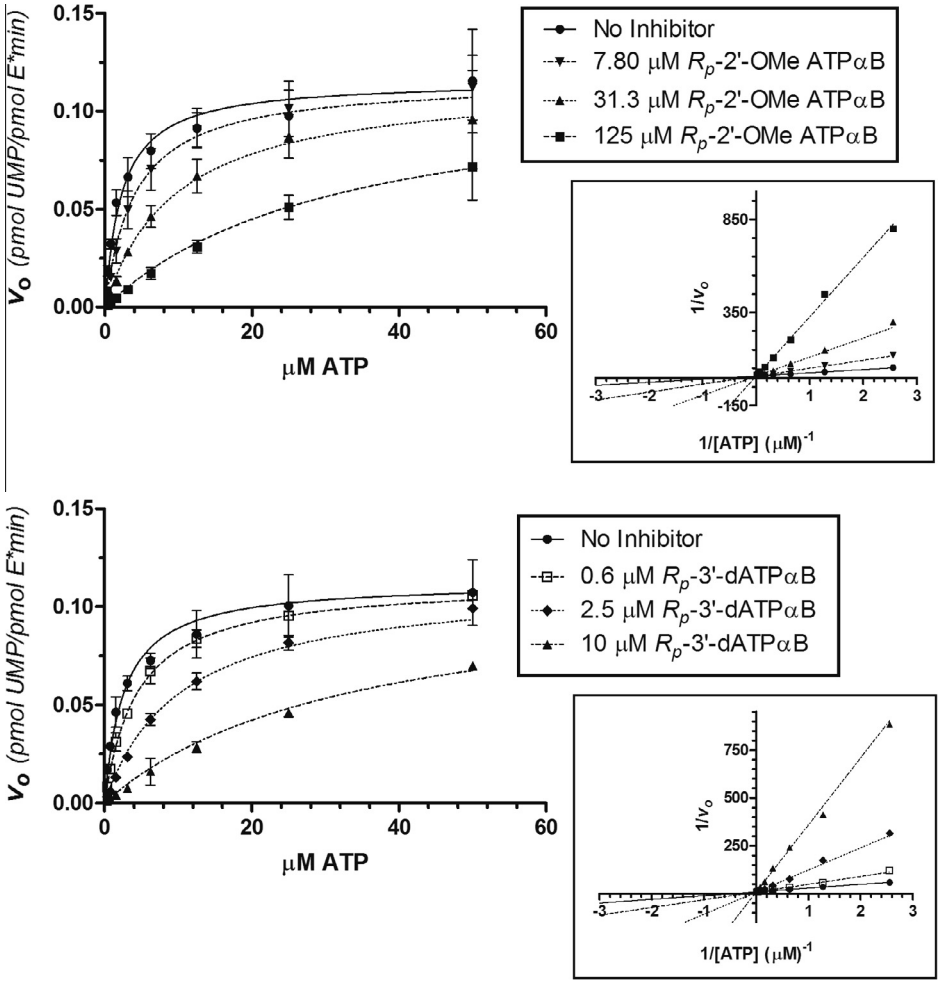

Fig. 8. Velocity curves fit to a competitive mechanism for (A) R_p-2′-O-Me ATPαB, **5a** and (B) R_p-3′-dATPαB, **5b.** Reactions were run parallel with natural phosphate controls and the K_i for each compound was determined from the mean of at least three independents experiments**.** Inset graphs are Lineweaver–Burk double-reciprocal plots showing convergent maximum reaction velocities (*y*-intercept)**.**

Table 3
Inhibition constant (K_i) determined for ATPαB inhibitors **5a**, and **5b** compared to NTP controls.

Nucleotide	K_i (μM)	K_m (μM)	K_i/K_m(ATP)	Potency Shift[a]
R_p-2′-O-Me ATPαB, **5a** (n = 3)	10.3 ± 1.41	-	5.07	5.2
2′-O-Me ATP (n = 3)	53.4 ± 2.80	-	26.3	-
R_p-3′-dATPαB, **5b** (n = 4)	0.882 ± 0.219	-	0.43	21
3′-dATP (n = 3)	18.7 ± 2.9	-	9.21	-
ATP (n = 10)	-	2.03 ± 0.395	-	-

[a] Potency shift is the ratio of the inhibition constant (K_i) of the normal phosphate control divided by the K_i of the NTPαB inhibitor.

than our experiments ($K_i/K_{m(ATP)}$ = 9.2). Interestingly enough, their single nucleotide incorporation assay, which more resembles *de novo* initiation than elongation, yielded much higher K_m values, ranging from 67 to 250 μM for the natural NTPs and lower apparent affinity ratios (0.8–1.6) showing less 3′-deoxy discrimination. This may indicate that the type of RNA template and assay used can affect how the enzyme discriminates between natural nucleotides and nucleotide analogs.

The type of total nucleotide incorporation assay used in our study shows the global effects of an inhibitor on RNA elongation in a system where the rate-limiting step is thought to be the dissociation of the enzyme from the full length product. The inhibitor most likely competes with all four natural NTPs at multiple sites in the genomic RNA, giving results that more closely resemble the virus' natural replicative process. To determine the actual binding constant (K_d), and polymerization rate constant (k_{pol}) of an incoming NTP, single nucleotide incorporation under pre-steady-state conditions would have to be utilized (Jin et al., 2012; Powdrill et al., 2011).

The effect of this α-*P*-BH_3 substitution on the kinetics of NS5B-catalyzed RNA chain elongation appears to increase the catalytic efficiency of both ATP and sugar-modified ATP analogues. This rate enhancement is likely due to a number of electronic and steric effects resulting from the borane group substitution: (a) the lower electronegativity of boron relative to oxygen allows the α-phosphorus to retain more electron density and become less positive, thus making the pyrophosphate (PP*i*) a better leaving group (Summers et al., 1998; Thatcher and Campbell, 1993); (b) the non-bridging oxygen opposite to the borane group retains slightly more electron density (compared with a normal phosphate) and coordi-

nates better to cations (Deval et al., 2005; Summers et al., 1998); and (c) the borane is isosteric to a methyl group and has a preference for hydrophobic environments (Summers et al., 1998), both of which may contribute to faster PP*i* loss due to coulombic repulsion. To our knowledge, these data represent the first time a phosphate modified NTP has been studied as a substrate for HCV NS5B RdRP.

These findings could have widespread applications given the range of sugar modified NS5B inhibitors that are currently being investigated. Existing viral RdRP inhibitors might be "retro-fitted" with the boranophosphate modification, in combination with a monophosphate prodrug strategy (Bobeck et al., 2010; Li et al., 2007; Shaw et al., 2000), in order to increase potency. Overall, this discovery could open up a larger avenue of thought in terms of future HCV therapeutic development (and possibly other RNA viruses as well).

Acknowledgements

We would like to thank Dr. Steven Carroll, Dr. David Olsen, Dr. Steven W. Ludmerer, Dr. Licia Tomei, and Merck & Co., Inc. for providing the HCV NS5BΔ55 polymerase and t500 RNA template and helpful discussions. This work was supported by National Institutes of Health grant R01-AI-52061.

Appendix A. Supplementary data

Supplementary data associated with this article can be found, in the online version, at http://dx.doi.org/10.1016/j.antiviral.2013.02.014.

References

Behrens, S.E., Tomei, L., De Francesco, R., 1996. Identification and properties of the RNA-dependent RNA polymerase of hepatitis C virus. EMBO J. 15, 12–22.
Bobeck, D.R., Schinazi, R.F., Coats, S.J., 2010. Advances in nucleoside monophosphate prodrugs as anti-HCV agents. Antivir. Ther. 15, 935–950.
Brautigam, C.A., Steitz, T.A., 1998. Structural and functional insights provided by crystal structures of DNA polymerases and their substrate complexes. Curr. Opin. Struct. Biol. 8, 54–63.
Bressanelli, S., Tomei, L., Rey, F.A., De Francesco, R., 2002. Structural analysis of the hepatitis C virus RNA polymerase in complex with ribonucleotides. J. Virol. 76, 3482–3492.
Bressanelli, S., Tomei, L., Roussel, A., Incitti, I., Vitale, R.L., Mathieu, M., De Francesco, R., Rey, F.A., 1999. Crystal structure of the RNA-dependent RNA polymerase of hepatitis C virus. Proc. Natl. Acad. Sci. 96, 13034–13039.
Bryant, F.R., Johnson, K.A., Benkovic, S.J., 1983. Elementary steps in the DNA polymerase I reaction pathway. Biochemistry 22, 3537–3546.
Carroll, S.S., Ludmerer, S., Handt, L., Koeplinger, K., Zhang, N.R., Graham, D., Davies, M.-E., MacCoss, M., Hazuda, D., Olsen, D.B., 2009. Robust antiviral efficacy upon administration of a nucleoside analog to hepatitis C virus-infected chimpanzees. Antimicrob. Agents Chemother. 53, 926–934.
Carroll, S.S., Sardana, V., Yang, Z., Jacobs, A.R., Mizenko, C., Hall, D., Hill, L., Zugay-Murphy, J., Kuo, L.C., 2000. Only a small fraction of purified hepatitis C RNA-dependent RNA polymerase is catalytically competent: implications for viral replication and in vitro assays. Biochemistry 39, 8243–8249.
Carroll, S.S., Tomassini, J.E., Bosserman, M., Getty, K., Stahlhut, M.W., Eldrup, A.B., Bhat, B., Hall, D., Simcoe, A.L., LaFemina, R., Rutkowski, C.A., Wolanski, B., Yang, Z., Migliaccio, G., De Francesco, R., Kuo, L.C., MacCoss, M., Olsen, D.B., 2003. Inhibition of hepatitis C virus RNA replication by 2′-modified nucleoside analogs. J. Biol. Chem. 278, 11979–11984.
Cheng, Y.-C., Prusoff, W.H., 1973. Relationship between the inhibition constant (K_I) and the concentration of inhibitor which causes 50 percent inhibition (I50) of an enzymatic reaction. Biochem. Pharmacol. 22, 3099–3108.
De Clercq, E., 2009. Anti-HIV drugs: 25 compounds approved within 25 years after the discovery of HIV. Int. J. Antimicrob. Agents 33, 307–320.
De Francesco, R., Behrens, S.-E., Tomei, L., Altamura, S., Jiricny, J., 1996. [4] RNA-dependent RNA polymerase of hepatitis C virus. Methods Enzymol. 275, 58–67.
Deval, J., Alvarez, K., Selmi, B., Bermond, M., Boretto, J., Guerreiro, C., Mulard, L., Canard, B., 2005. Mechanistic insights into the suppression of drug resistance by human immunodeficiency virus type 1 reverse transcriptase using alpha-boranophosphate nucleoside analogs. J. Biol. Chem. 280, 3838–3846.
Deval, J., Powdrill, M.H., D'Abramo, C.M., Cellai, L., Gotte, M., 2007. Pyrophosphorolytic excision of nonobligate chain terminators by hepatitis C virus NS5B polymerase. Antimicrob. Agents Chemother. 51, 2920–2928.
Dobrikov, M., Shaw, B.R., 2005. Molecular mechanism for suppression of drug-resistant MMLV-revers transcriptaseby (α-*P*-borano)-2′,3′-dideoxycitidine-5′-triphosphate. Antivir. Res. 65, A52.
Dobrikov, M.I., Sergueeva, Z.A., Shaw, B.R., 2003. Incorporation of (α-P-Borano)-2′,3′-dideoxycytidine 5′-triphosphate into DNA by drug-resistant MMLV reverse transcriptase and Taq DNA polymerase. Nucleosides Nucleotides Nucleic Acids 22, 1651–1655.
Eldrup, A.B., Allerson, C.R., Bennett, C.F., Bera, S., Bhat, B., Bhat, N., Bosserman, M.R., Brooks, J., Burlein, C., Carroll, S.S., Cook, P.D., Getty, K.L., MacCoss, M., McMasters, D.R., Olsen, D.B., Prakash, T.P., Prhavc, M., Song, Q., Tomassini, J.E., Xia, J., 2004. Structure-activity relationship of purine ribonucleosides for inhibition of hepatitis C virus RNA-dependent RNA polymerase. J. Med. Chem. 47, 2283–2295.
Fried, M.W., Shiffman, M.L., Reddy, K.R., Smith, C., Marinos, G., Gonçales, F.L., Häussinger, D., Diago, M., Carosi, G., Dhumeaux, D., Craxi, A., Lin, A., Hoffman, J., Yu, J., 2002. Peginterferon Alfa-2a plus ribavirin for chronic hepatitis C virus infection. N. Engl. J. Med. 347, 975–982.
Ghany, M.G., Nelson, D.R., Strader, D.B., Thomas, D.L., Seeff, L.B., 2011. An update on treatment of genotype 1 chronic hepatitis C virus infection: 2011 practice guideline by the American Association for the Study of Liver Diseases. Hepatology 54, 1433–1444.
He, K., Hasan, A., Krzyzanowska, B., Shaw, B.R., 1998. Synthesis and separation of diastereomers of ribonucleoside 5′-(α-P-Borano)triphosphates. J. Org. Chem. 63, 5769–5773.
Jin, Z., Leveque, V., Ma, H., Johnson, K.A., Klumpp, K., 2012. Assembly, purification, and pre-steady-state kinetic analysis of active RNA-dependent RNA polymerase elongation complex. J. Biol. Chem. 287, 10674–10683.
Li, P., Sergueeva, Z.A., Dobrikov, M., Shaw, B.R., 2007. Nucleoside and oligonucleoside boranophosphates: chemistry and properties. Chem. Rev. 107, 4746–4796.
Lohmann, V., Korner, F., Herian, U., Bartenschlager, R., 1997. Biochemical properties of hepatitis C virus NS5B RNA-dependent RNA polymerase and identification of amino acid sequence motifs essential for enzymatic activity. J. Virol. 71, 8416–8428.
Meyer, P., Schneider, B., Sarfati, S., Deville-Bonne, D., Guerreiro, C., Boretto, J., Janin, J., Veron, M., Canard, B., 2000. Structural basis for activation of α-boranophosphate nucleotide analogues targeting drug-resistant reverse transcriptase. EMBO J. 19, 3520–3529.
Mosley, R.T., Edwards, T.E., Murakami, E., Lam, A.M., Grice, R.L., Du, J., Sofia, M.J., Furman, P.A., Otto, M.J., 2012. Structure of hepatitis C virus polymerase in complex with primer-template RNA. J. Virol. 86, 6503–6511.
Murakami, E., Bao, H., Ramesh, M., McBrayer, T.R., Whitaker, T., Micolochick Steuer, H.M., Schinazi, R.F., Stuyver, L.J., Obikhod, A., Otto, M.J., Furman, P.A., 2007. Mechanism of activation of beta-D-2′-deoxy-2′-fluoro-2′-C-methylcytidine and inhibition of hepatitis C virus NS5B RNA polymerase. Antimicrob. Agents Chemother. 51, 503–509.
O'Farrell, D., Trowbridge, R., Rowlands, D., Jäger, J., 2003. Substrate complexes of hepatitis C virus RNA polymerase (HC-J4): structural evidence for nucleotide import and de-novo initiation. J. Mol. Biol. 326, 1025–1035.
Olsen, D.B., Eldrup, A.B., Bartholomew, L., Bhat, B., Bosserman, M.R., Ceccacci, A., Colwell, L.F., Fay, J.F., Flores, O.A., Getty, K.L., Grobler, J.A., LaFemina, R.L., Markel, E.J., Migliaccio, G., Prhavc, M., Stahlhut, M.W., Tomassini, J.E., MacCoss, M., Hazuda, D.J., Carroll, S.S., 2004. A 7-deaza-adenosine analog is a potent and selective inhibitor of hepatitis C virus replication with excellent pharmacokinetic properties. Antimicrob. Agents Chemother. 48, 3944–3953.
Penin, F., Dubuisson, J., Rey, F.A., Moradpour, D., Pawlotsky, J.-M., 2004. Structural biology of hepatitis C virus. Hepatology 39, 5–19.
Powdrill, M.H., Bernatchez, J.A., Götte, M., 2010. Inhibitors of the hepatitis C virus RNA-dependent RNA polymerase NS5B. Viruses 2, 2169–2195.
Powdrill, M.H., Tchesnokov, E.P., Kozak, R.A., Russell, R.S., Martin, R., Svarovskaia, E.S., Mo, H., Kouyos, R.D., Götte, M., 2011. Contribution of a mutational bias in hepatitis C virus replication to the genetic barrier in the development of drug resistance. Proc. Natl. Acad. Sci. 108, 20509–20513.
Sangiovanni, A., Prati, G.M., Fasani, P., Ronchi, G., Romeo, R., Manini, M., Del Ninno, E., Morabito, A., Colombo, M., 2006. The natural history of compensated cirrhosis due to hepatitis C virus: a 17-year cohort study of 214 patients. Hepatology 43, 1303–1310.
Selmi, B., Boretto, J., Sarfati, S.R., Guerreiro, C., Canard, B., 2001. Mechanism-based Suppression of dideoxynucleotide resistance by K65R human immunodeficiency virus reverse transcriptase using an α-boranophosphate nucleoside analogue. J. Biol. Chem. 276, 48466–48472.
Shaw, B.R., Dobrikov, M., Wang, X.I.N., Wan, J., He, K., Lin, J.-L., Li, P., Rait, V., Sergueeva, Z.A., Sergueev, D., 2003. Reading, writing, and modulating genetic information with boranophosphate mimics of nucleotides, DNA, and RNA. Ann. NY. Acad. Sci. 1002, 12–29.
Shaw, B.R., Sergueev, D., He, K., Porter, K., Summers, J., Sergueeva, Z., Rait, V., Phillips, M.I., 2000. Boranophosphate backbone: a mimic of phosphodiesters, phosphorothioates, and methyl phosphonates. In: Methods Enzymology. Academic Press, pp. 226–257.
Shim, J., Larson, G., Lai, V., Naim, S., Wu, J.Z., 2003. Canonical 3′-deoxyribonucleotides as a chain terminator for HCV NS5B RNA-dependent RNA polymerase. Antivir. Res. 58, 243–251.
Sofia, M.J., Chang, W., Furman, P.A., Mosley, R.T., Ross, B.S., 2011. Nucleoside, nucleotide, and non-nucleoside inhibitors of hepatitis C virus NS5B RNA-dependent RNA-polymerase. J. Med. Chem. 55, 2481–2531.

Sood, A., Shaw, B.R., Spielvogel, B.F., 1990. Boron-containing nucleic acids. 2. Synthesis of oligodeoxynucleoside boranophosphates. J. Am. Chem. Soc. 112, 9000–9001.

Summers, J.S., Hoogstraten, C.G., Britt, R.D., Base, K., Shaw, B.R., Ribeiro, A.A., Crumbliss, A.L., 2001. ^{31}P NMR probes of chemical dynamics: paramagnetic relaxation enhancement of the ^{1}H and ^{31}P NMR resonances of methyl phosphite and methylethyl phosphate anions by selected metal Complexes. Inorganic Chem. 40, 6547–6554.

Summers, J.S., Roe, D., Boyle, P.D., Colvin, M., Shaw, B.R., 1998. structural studies of a borane-modified phosphate diester linkage: ab initio calculations on the dimethylboranophosphate anion and the single-crystal X-ray structure of its diisopropylammonium salt. Inorganic Chem. 37, 4158–4159.

Takamizawa, A., Mori, C., Fuke, I., Manabe, S., Murakami, S., Fujita, J., Onishi, E., Andoh, T., Yoshida, I., Okayama, H., 1991. Structure and organization of the hepatitis C virus genome isolated from human carriers. J. Virol. 65, 1105–1113.

Thatcher, G.R.J., Campbell, A.S., 1993. Phosphonates as mimics of phosphate biomolecules: ab initio calculations on tetrahedral ground states and pentacoordinate intermediates for phosphoryl transfer. J. Organic Chem. 58, 2272–2281.

Westman, E., Strömberg, R., 1994. Removal of t-butyldimethylsilyl protection in RNA-synthesis. Triethylamine trihydrofluoride (TEA, 3HF) is a more reliable alternative to tetrabutylammonium fluoride (TBAF). Nucleic Acids Res. 22, 2430–2431.

WHO, 1999. Hepatitis C – global prevalence (update). Weekly Epidemiological Record 74, 425–427.